Hindawi Publishing Corporation
Journal of Sensors
Volume 2016, Article ID 9379203, 11 pages
http://dx.doi.org/10.1155/2016/9379203

Research Article

Comparison and Calibration of Mobile Phone Fisheye Lens and Regular Fisheye Lens via Equidistant Model

Cumhur Sahin

Department of Geodetic and Photogrammetric Engineering, Faculty of Engineering, Gebze Technical University, PK 141, Gebze, 41400 Kocaeli, Turkey

Correspondence should be addressed to Cumhur Sahin; csahin@gyte.edu.tr

Received 25 December 2015; Revised 28 February 2016; Accepted 7 March 2016

Academic Editor: Guiyun Tian

Copyright © 2016 Cumhur Sahin. This is an open access article distributed under the Creative Commons Attribution License, which permits unrestricted use, distribution, and reproduction in any medium, provided the original work is properly cited.

Nowadays, mobile phones are more than a device that can only satisfy the communication need between people. In addition to providing ease to human lives with various applications, lens kits that can be integrated to mobile phones have recently been introduced. Fisheye lenses that are compliant with mobile phones are one of these new types of equipment. Since fisheye lenses integrated with mobile phones are lightweight and easy to use, they are advantageous. In addition to this advantage, whether fisheye lens and mobile phone combination can be used in a photogrammetric way is experimented, and if so, what will be the result. The main purpose of this study is to test fisheye lens equipment used with mobile phones. In this study, standard calibration of "Olloclip 3 in one" fisheye lens used with iPhone 4S mobile phone and "Nikon FC-E9" fisheye lens used with Nikon Coolpix8700 are compared based on equidistant model. The results of these calibrations are analyzed, using photogrammetric bundle block adjustment. This study suggests a precalibration process of these kinds of hardware for the photogrammetric process in the test field.

1. Introduction

While mobile phones are mainly used for outdoors communication, the developing electronics technology enabled them to be used for various other applications on the Globe as well. Classical lens kit is one of the samples that have long been mounted to mobile phones giving people the opportunity to take pictures and share transiently. Recently, state-of-the-art technology product fisheye lenses which have been integrated with mobile phones are one of these new types of equipment. These types of equipment are lightweight and easy to use. Additionally, these lenses are cost efficient compared to conventional fisheye lenses. Some of those lens kits for iPhone are presented in [1]. The characteristics of Olloclip lens used in this paper are presented in [2]. Cameras on mobile phones are as capable as compact cameras that we use in our daily lives. Today, people do not want to possess a digital camera since mobile phones are equipped with enough capable cameras. There are studies which examine whether mobile phone cameras can be used in photogrammetric studies. Reference [3] reports first experiences in calibration and accuracy validation of mobile phone cameras. In [4], building facades are captured with mobile phone cameras and digital cameras and the obtained images are converted into vertical plane with Pictran, PhotoModeler, and PhoTopol photogrammetric software. Reference [5] confirmed the advantages of the proposed system by evaluation experiments. The new system will be able to contribute to the novel mobile Web map services with fisheye views for mobile terminals such as cellular phones.

Fisheye lenses provide instant wide angle images from one point with a single camera. Fisheye optics are placed onto CCD (Charge Couple Device) or CMOS (Complementary Metal Oxide Semiconductor) cameras without needing any complex technology. They do not require an external mirror or rotational device. Thus, these optics are small in size and do not require any maintenance [6]. They have a very short focal length, which produces a hemisphere [7]. Fisheye lenses allow imaging a large sector of the surrounding space by a single photo; therefore, they are useful for several applications. Besides the pure visualization of landscapes or interiors (e.g., ceiling frescos in historical buildings) for advertisement or

internet presentations, fisheye images can also be used for measurement tasks [8]. The first fisheye lens has been created by R. Hill in 1924 [9], but they have not been preferred in photogrammetric measurements since they provide images with huge distortions and they do not meet central projection. Using the images obtained from fisheye lens imaging systems in photogrammetric measurement and modeling processes becomes popular in recent years by the help of the development in software and hardware technologies. Lately, a significant increase has been seen in terms of volume scientific research on this subject matter. Recently, there have been several academic studies presenting the benefit from fisheye lenses. Fisheye cameras are finding increasing number of applications in surveillance, robotic vision, automotive rear-view imaging systems, and so forth, because of their wide angle properties [10]. Fisheye lens cameras have also been used during sky observations [11], visual sun compass creation [12], and sun path diagram derivation [13]. A novel panoramic imaging system uses a curved mirror as a simple optical attachment to a fisheye lens [14]. Reference [15] describes a visual markerless real-time tracking system for Augmented Reality applications. The system uses a FireWire camera with a fisheye lens mounted at 10 fps. Reference [16] presents a new Mobile Mapping System mounted on a vehicle to reconstruct outdoor environment in real time. Reference [17] presents a cooperative approach for tracking a moving spherical object in three-dimensional space by a team of mobile robots equipped with sensors, in a highly dynamic environment. Reference [18] explores the use of a fisheye camera to achieve the scene tunnel acquisition. In [19] the authors have focused on dioptric systems to implement a robot surveillance application for fast and robust tracking of moving objects in dynamic, unknown environments. Another application that uses fisheye lens is a research which examines the use of fisheye lenses as optical sensors on Unmanned Aerial Vehicle (UAV) platform in Queensland Technical University in Australia [20]. Reference [21] uses a fisheye camera for horizon detection in aerial images. Reference [22] proposes three-dimensional measurement method of underwater objects using a fisheye stereo camera. In [23], a novel technique to accurately estimate the global position of a moving car using an omnidirectional camera and untextured three-dimensional city model is proposed. Today, one of the areas that most frequently benefit from fisheye lenses are applications done in combination with terrestrial laser scanners. Reference [24] presents a comparison of automatic photogrammetric techniques to terrestrial laser scanning for three-dimensional modeling of complex interior spaces. The 8 mm fisheye lens that was used allowed us to acquire photos with a global view of the scene and thus with textured zones in every image, which is essential for the Scale Invariant Feature Transform (SIFT) algorithm. Reference [25] presents the integration of a geometric model of fisheye lenses and a geometric terrestrial laser scanner model in a bundle block adjustment.

Fisheye projection functions are designed such that a greater portion of the scene is projected onto the image sensor on the image plane, at the expense of introducing (often considerable) radial distortion [26]. The fisheye lens camera should be calibrated to be used in applications that require high accuracy [27]. There are different studies in literature which focus on the calibration of fisheye lenses. Reference [6] presented rigorous mathematical models for the calibration of a stereo system composed of two fisheye lens cameras and for the epipolar rectification of the images acquired by this dual system. Reference [28] presented the calibration of a Kodak DSC 14 Pro with Nikkor 8 mm fisheye lens, which follows the equidistant projection. The rigorous mathematical models based on stereographic, equidistant, orthogonal, and equisolid angle projections were used in combination with symmetric radial, decentering, and affinity distortion models. Reference [29] proposes a generic camera model, which is suitable for fisheye lens cameras as well as for conventional and wide angle lens cameras, and a calibration method for estimating the parameters of the model. Fisheye lenses are not perspective lenses, image resolution in these lenses is not fixed (univocal), and illumination is not distributed homogeneously [30]. In photogrammetry, the collinearity mathematical model, based on perspective projection combined with lens distortion models, is generally used in the camera calibration process. However, fisheye lenses are designed for the following different spherical projections models such as stereographic, equidistant, orthogonal, and equisolid angle [27]. The technical construction of most fisheye lenses complies with the equidistant or equisolid angle projection. Diagonal fisheye lenses are mainly constructed following the equisolid angle projection geometry, where the distortion in the image edges is more significant in comparison to fisheye lenses with the equidistant projection. The orthographic projection geometry can only be realized with a sophisticated optical construction. Stereographic projection is not practically realizable [28]. Among the other models proposed, an important one is the equidistant model. The model proposes that the distance between an image point and the center of radial distortion is proportional to the angle between a corresponding three-dimensional point, the optical center, and the optical axis [31]. Equidistant fisheye lenses are often used for scientific measurement where the measurement of angles is necessary. Thus, it is also sometimes referred to as an equiangular fisheye lens [32].

The main purpose of this study is to test fisheye lens equipment used with mobile phones. Mobile phone imaging with the additional hardware has been used more popularly not only outside but also indoor applications. Therefore, hardware properties of this wide angle optics will be used in the photogrammetric documentation in the near future for mobile phone imaging. Since fisheye lenses integrated with mobile phones are lightweight and easy to use, they are advantageous. In addition to this advantage, it is experimented whether fisheye lens and mobile phone combination can be used in a photogrammetric way, and if so, what will be the result. In this study, standard calibration of "Olloclip 3 in one" fisheye lens used with iPhone 4S mobile phone and "Nikon FC-E9" fisheye lens used with Nikon Coolpix8700 are compared based on equidistant model. The results of these calibrations are analyzed, using photogrammetric bundle block adjustment. Geometric properties of this wide angle lenses will be more important in the photogrammetric

measurement assessment. This study suggests a precalibration process of these kinds of hardware for the photogrammetric process in the test field. In the literature, although there are many geometric camera calibration publications, none of them compares the mobile phone fisheye lens kit with conventional fisheye lens on the fundamentals of photogrammetric measurement assessment. The results of this photogrammetric process are also compared with conventional wide angle hardware in this paper.

Section 2 of this paper briefly describes equidistant model. Section 3 reports an empirical study for calibration of the combination of iPhone 4S camera with Olloclip 3 in one fisheye lens and Nikon Coolpix8700 camera FC-09 fisheye lens combination by using equidistant model. Section 4 interprets the results which are outcome from the experiment process. In Section 5, the advantages and disadvantages have been explained according to the obtained results for iPhone 4S camera with Olloclip 3 in one fisheye lens.

2. Equidistant Projection Function for Fisheye Lenses

The perfect fisheye lens can be modeled as a sphere through which scene projections are described by two basic properties. First, the field of view encompasses 2π steradians and produces a circular image so that distortions are symmetrical about the image center. Second, the fisheye lens possesses an infinite depth-of-field in that all objects in the image are in focus. Furthermore, the formation of nonlinear image distortion is governed by two postulates, the azimuth angle invariability and the equidistant projection rule. These postulates describe the projection of object points onto the sensor and will directly affect the dewarping algorithm that will be subsequently developed [33].

The first postulate is that the azimuth angle invariability governs the projection of points lying in the plane that passes through the optical axis perpendicular to the sensor plane. The azimuth angle of the object points and their projections onto the sensor remain unchanged due to differences in the object distance or elevation within the content plane [33]. According to [34], the equidistant lens is "preferable for measurement of incidence angles (θ) and azimuth angles. The effect of error of lens position is small, and the linear relation of radial distance (r_d) and incidence angle (θ) of a ray from the three-dimensional point is convenient to analyze".

The equidistant projection rule, the second postulate, describes the relationship between the radial distance (r_d) of an image point in the sensor plane to the zenith (incidence, (θ)) angle created by the vector from the image center to the world object point as defined in Figure 1. This rule states that for a spherical lens a linear relationship exists between the center to image point radial distance, r_d, and the zenith angle, (θ) [33].

As the zenith angle varies from 0 to 90 degrees, the radial distance of the corresponding image point varies linearly from 0 to a maximum value R, determined by the modeled sphere's radius [33].

In equidistant projection, the radial distance (r_d) on the image plane is directly proportional to the angle of the incident ray and is equivalent to the length of the arc segment between the z-axis and the projection ray of point P on the sphere Figure 2 [26].

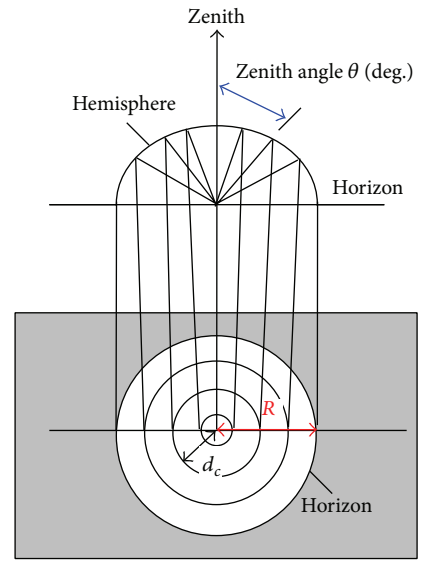

Figure 1: Equidistant projection (equidistant projection, $\theta/90 = d_c/R$) [35].

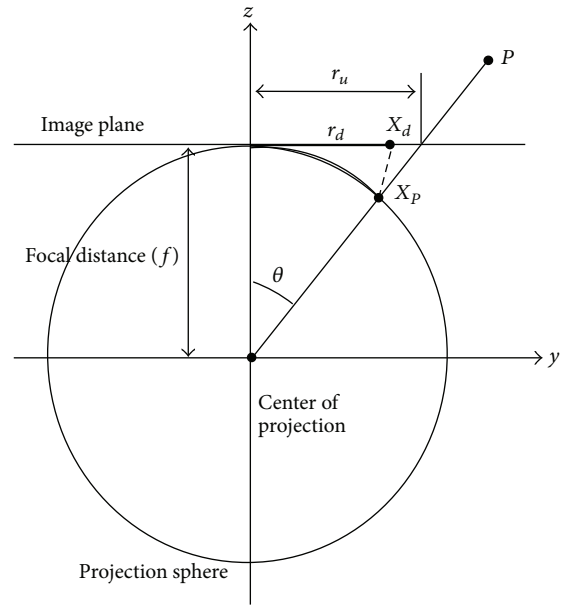

Figure 2: Equidistant fisheye projection function representation.

Thus, the equidistant projection function is given as follows:

$$r_d = f \cdot \theta, \tag{1}$$

where r_d is the fisheye radial distance of a projected point from the center, f is focal distance, and θ is the incidence angle of a ray from the three-dimensional point being projected to the image plane. This is one of the more common mapping functions that fisheye cameras are designed to

follow, the others being the stereographic, equisolid, and orthogonal mapping functions [36]. Equation (2) is derived by substituting arctangent function for θ in (1), where r_u is the height of the projection on the image plane (the subscript u being used to denote the undistorted projection) [32]:

$$r_d = f \cdot \arctan\left(\frac{r_u}{f}\right). \tag{2}$$

In equidistant projection model, the angle of the projected ray in radians translates linearly to the distorted radial distance on the image plane. Additionally, the projected distorted distance r_d is equivalent to the length of the arc segment between the z-axis and X_P, which is the point of intersection of the projection ray of point X with the projection sphere [32].

Most real optical systems have some undesirable effects, rendering the assumption of the pinhole camera model inaccurate. The significant evident of these effects is radial barrel distortion, particularly noticeable in fisheye camera systems, where the level of this distortion is relatively extreme [26]. For normal and narrow field of view (FOV) cameras, the effects of radial distortion can be considered negligible for most application. However, in wide angle and fisheye cameras, radial distortion can cause severe problems, not only visually but for further processing in computer vision applications such as object detection, recognition, and classification [32]. Radial lens distortion causes points on the image plane to be displaced in a nonlinear fashion from their ideal position in the rectilinear pinhole camera model, along a radial axis from the distortion center in the equidistant image plane. The visual effect of this displacement in fisheye optics is that the image will have a higher resolution in the foveal areas, with the resolution decreasing nonlinearly towards the peripheral areas of the image [37].

For additional parameters to compensate for deviations of the geometric fisheye model from the physical reality, the same parameters are applied as they are in common use for central perspective lenses [28]. Accordingly the equidistant projection function with additional parameters is given as follows:

$$r_d = f \cdot \arctan\left(\frac{r_u}{f}\right) + \text{Additional Parameters}. \tag{3}$$

Due to the particularly high levels of distortion present in fisheye cameras, there have been several alternative models developed [37]. Some models are Fisheye Transform, field of view, Division Model, and Polynomial Model [38]. The work in [28] investigates the addition of the Brown parameters to the basic geometric fisheye model to compensate for the remaining "systematic effects" [38].

To describe the projection of an object point into a hemispherical fisheye lens image, three coordinate system are used. The superordinated cartesian object coordinate system (X, Y, Z) and the camera coordinate system (x, y, z) in Figure 3. The image coordinate system (x', y') is defined as usual in photogrammetric applications, which means the origin is the image center, and the x'-axis and y'-axis are parallel with the x-axis and y-axis of camera

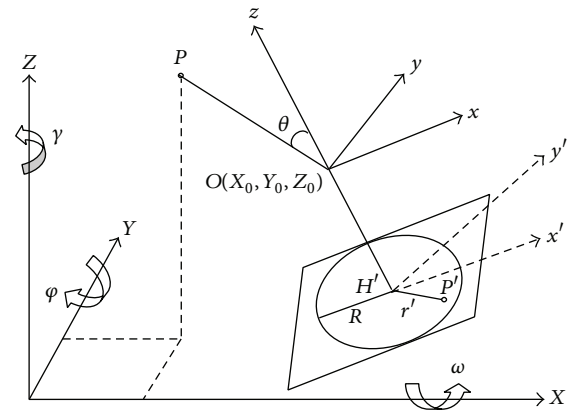

Figure 3: Geometrical model of a fisheye camera.

coordinate system [28]. The geometric concept is based on the dependence of the image radius r' and the angle of incidence θ [25].

Object coordinates are transformed into the camera coordinate system. One has (4), where X is the coordinate vector in the object coordinate system; x is the coordinate vector in the camera coordinate system; R is the rotation matrix and X_0 the translation between object and camera coordinate system:

$$x = R^{-1}\left(X - X_0\right). \tag{4}$$

The incidence angle θ in the camera coordinate system is defined as follows:

$$\tan\theta = \frac{\sqrt{x^2 + y^2}}{z}. \tag{5}$$

Instead of functions for the image radius r', functions for the image coordinates x' and y' are required. For this purpose (6) is applied:

$$r' = \sqrt{x'^2 + y'^2}. \tag{6}$$

After transformations of the equations are described above, the final fisheye projection equations for the image coordinates are derived.

The model equations are finally extended by the coordinates of the principal point x_0' and y_0' (see (7)) and the correction terms $\Delta x'$ and $\Delta y'$ (see (8) and (9)) which contain additional parameters to compensate for systematic effects.

Equidistant projection:

$$x' = c \cdot \frac{\arctan\left(\sqrt{x^2 + y^2}/z\right)}{\sqrt{(y/x)^2 + 1}} + x_0' + \Delta x',$$

(a) (b)

Figure 4: Camera fisheye equipment used in application ((a) is iPhone 4S with Olloclip 3 in one; (b) is Nikon Coolpix8700 with FC-09 fisheye lenses).

$$y' = c \cdot \frac{\arctan\left(\sqrt{x^2 + y^2}/z\right)}{\sqrt{(x/y)^2 + 1}} + y'_0 + \Delta y', \tag{7}$$

$$\Delta x = x' \cdot \left(A_1 r'^2 + A_2 r'^4 + A_3 r'^6\right) + B_1 \cdot \left(r'^2 + 2x'^2\right) + 2B_2 x' y' + C_1 \cdot x' + C_2 \cdot y', \tag{8}$$

$$\Delta_y = y' \cdot \left(A_1 r'^2 + A_2 r'^4 + A_3 r'^6\right) + 2B_1 x' y' + B_2 \cdot \left(r'^2 + 2y'^2\right), \tag{9}$$

where; A_1, A_2, and A_3 are radial distortion parameters. B_1 and B_2 are decentric distortion parameters. C_1 and C_2 are horizontal scale factor and shear factor. c is the camera constant which equals focal distance.

Table 1: Technical specifications of the cameras.

	iPhone 4S	Nikon Coolpix8700
Sensor	CMOS 1/3.2″ sensor size	CCD 2/3″
Image resolution	3264 × 2448 (8.0 MP)	3264 × 2448 (8.0 MP)
*Focal length	4.324602 mm	9.027620 mm
*Pixel size	1.4 μm	2.7 μm
Digital zoom values	Up to 5x	Up to 4x
Aspect ratio	4 : 3	4 : 3; 3 : 2
LCD size	3.5″	1.8″

*These are the values obtained after separate calibrations performed before the application in PI3000 software for iPhone 4S and Nikon Coolpix8700 cameras used in the application. The pictures in the resolution of 3264 × 2448 are taken in this focal length.

3. Experiments

The characteristics of the cameras and fisheye lenses which were chosen for the application are given below.

Nikon Coolpix8700 digital camera has 8-megapixel resolution and CCD sensor. The 8x optical Zoom-Nikkor lens (f/2.8–4.2) offers a focal range of 8.9–71.2 mm [39]. Nikon FC-E9 fisheye lens: focal length of the camera's lens reduced to x0.2 provides approximately 183° (COOLPIX 5700)/190° (COOLPIX 5400) view angle [39].

iPhone 4S camera has 8-megapixel resolution and CMOS sensor. Its focal length is 35 mm [40]. Olloclip 3 in one fisheye lens: the Olloclip is a device providing three different lens options for iPhone; these are wide-angle, fisheye, and macro. The Olloclip with the fisheye lens acquires 180-degree field of view [41].

Application's camera fisheye lens combinations are shown in Figure 4 and also Table 1 shows technical specifications of the cameras used in the application.

The Olloclip 3 in one was mounted on the iPhone 4S. Images acquired with iPhone 4S and Olloclip 3 in one fisheye lens combination were captured with a focal distance of 4.28 mm. Images have 3264 × 2448 pixels and 1.4 μm pixel width.

The calibration field used in this study is a satellite antenna having 150 cm diameter with 112 control points on it. It was chosen since it has a smooth digital surface model and it is geometrically similar to the lens surface model. In this way, the analysis of the errors caused by the geometry of the objective and a balanced distribution of the depth differences over the image acquisition line on the surface model are accomplished. Point location accuracy is approximately 30–35 μm. In order to get the determined point location accuracy, a geodesic Wild T3 theodolite was chosen for direction measurements. In total, five serial measurements were made horizontally and vertically with Wild T3 [42]. Used calibration field is complying with self-calibration model which is a dish antenna model. Figure 5 shows the images of the calibration field taken by the two camera-lens combinations. The images of the calibration field were taken with the minimum focal length of each camera without zooming.

The application benefits from the comparison made over iPhone 4S Olloclip 3 in one camera fisheye lens combination

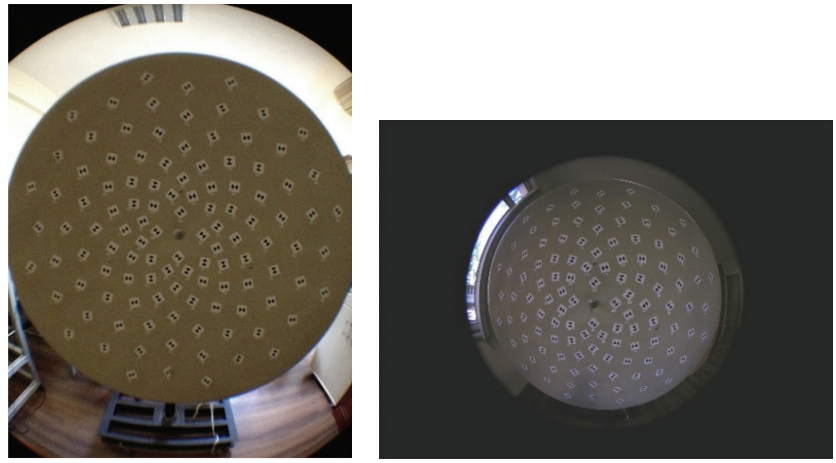

(a) (b)

Figure 5: Image of calibration field ((a) iPhone 4S camera with Olloclip 3 in one; (b) Nikon Coolpix8700 camera with Nikon FC-E9 fisheye lens).

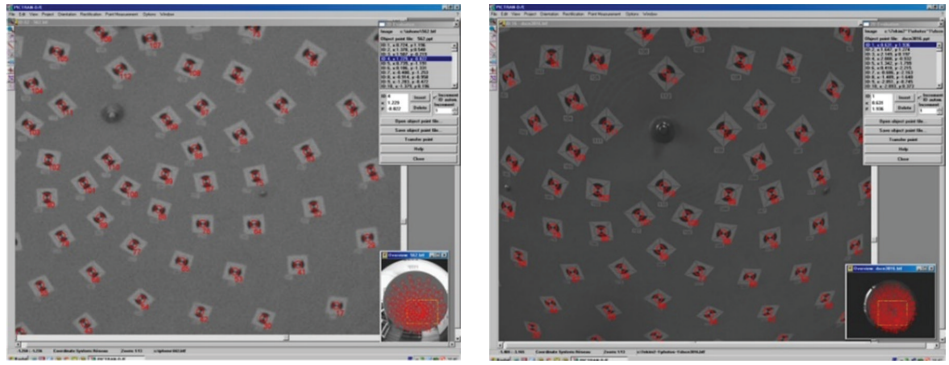

(a) (b)

Figure 6: Measurement of image coordinates of the fisheye lenses in Pictran D software ((a) taken from the combination of iPhone 4S camera with Olloclip 3 in one; (b) taken from the combination of Nikon Coolpix8700 camera with Nikon FC-E9 fisheye lens).

with Coolpix8700 camera FC-09 fisheye lens combination in terms of equidistant fisheye model (see (7)) which gives the best result in bundle block adjustment. In the application, the calibration values derived from equidistant fisheye model for iPhone 4S Olloclip 3 in one camera fisheye lens combination and Coolpix8700 camera FC-09 fisheye lens combination are compared. (See (8) and (9).) Equations use A_1, A_2, A_3, B_1, B_2, C_1, and C_2 coefficients as calibration parameters. Nine of 112 control points are considered passing points, while 103 of them are full control points. 13 images of calibration field were taken by iPhone 4S Olloclip 3 in one camera fisheye lens combination from different locations taking into consideration free network adjustment rules. The same procedure was also applied for Coolpix8700 camera FC-09 fisheye lens combination. After then, the two-dimensional image coordinates of 112 control points for 13 images were measured in Pictran D software for iPhone 4S Olloclip 3 in one camera fisheye lens combination. The same procedure was also applied for Coolpix8700 camera FC-09 fisheye lens combination. The measurements of the two-dimensional image coordinates in Pictran D software are shown in Figure 6.

Table 2: Calibration results of two different fisheye lenses in bundle adjustment software.

	iPhone 4S with Olloclip 3 in one	Nikon Coolpix8700 with Nikon FC-E9
Sigma0	0.00099	0.00163
Convergence	0	0
Maximum iteration	100	100
Required iteration	18	32
Calculation time	3.57 sn	6.41 sn
Unknown	396	396
Observations	2868	2838

The resulting image coordinates were evaluated in bundle block adjustment software developed by Dr. Danilo Schneider in Dresden Technical University in Germany. According to the bundle block adjustment results, Tables 2 and 3 were acquired.

Table 3: Calibration parameters calculated for equidistant model.

	iPhone 4S with Olloclip 3 in one (mm)			Nikon Coolpix8700 with Nikon FC-E9 (mm)		
	Value	Root mean square	Significance	Value	Root mean square	Significance
c_k	−2.23950000	0.00161000	8	−1.69005000	0.00203000	8
x_0	0.05886000	0.00397000	8	0.03987000	0.00259000	8
y_0	0.10471000	0.00399000	8	0.11442000	0.00240000	8
A_1	0.00080228	0.00027401	8	0.00118750	0.00038919	6
A_2	−0.00386240	0.00007329	8	−0.00067814	0.00005062	8
B_1	−0.00105490	0.00016903	8	−0.00026227	0.00012548	4
B_2	−0.00137450	0.00015347	8	0.00021274	0.00011927	3
C_1	0.00050562	0.00032783	1	−0.00009505	0.00029182	1
C_2	−0.00038251	0.00030980	6	0.00031644	0.00028458	1

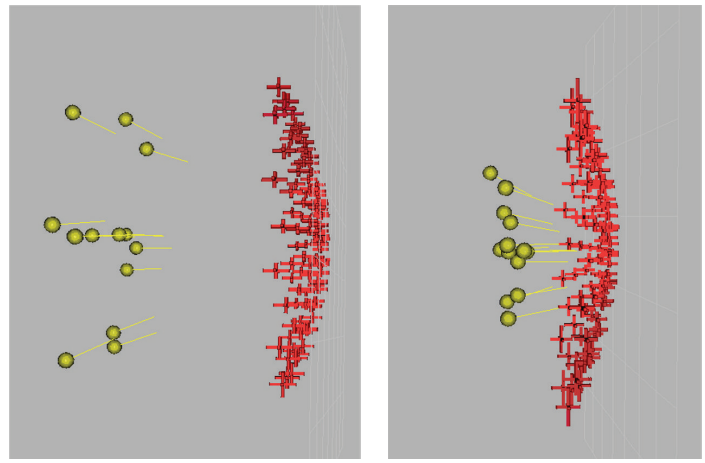

(a) (b)

Figure 7: Three-dimensional position of projection points with regard to antenna; three-dimensional coordinates of the camera as the result of balancing ((a) shows values for iPhone 4S camera with Olloclip 3 in one and (b) shows values for Nikon Coolpix8700 camera with Nikon FC-E9 fisheye lens).

The results of bundle block adjustment calculation by the software for 13 images captured with iPhone 4S camera and Olloclip 3 in one are given, respectively; the sigma0 value is 0.00099 and the pixel size is 0.0022 mm. The results of bundle block adjustment calculations by the software for 13 images captured with Nikon Coolpix8700 camera and FC-09 fisheye lens are given, respectively; the sigma0 value is 0.00163 and the pixel size is 0.0022 mm. Sigma0 is the root mean square of measurements for image coordinates after bundle block adjustment. Table 2 shows the resulting values in both of the calibrations. According to software's postadjustment outputs, additionally, projection point parameters (X_0, Y_0, Z_0 and omega, phi, kappa) of the 13 images and object points' significance for both the camera and lens combination are 8, which is 99.9 percent. (Software' significance values are 1—no significance, 2—80%, 3—90%, 4—95%, 5—98%, 6—99%, 7—99.8%, and 8—99.9% high significance.)

Figure 7 shows actual positions of three-dimensional coordinates of calibration field obtained by adjustment results and projection points of each of the 13 images that come from both of the calibration files acquired after adjustment.

4. Results

At the end of the application designed for testing, numerical values of calibration parameters and root mean square of those parameters that were calculated according to equidistant model were compared between the "Olloclip 3 in one" fisheye lens used with iPhone 4S mobile phone and standard "Nikon FC-E9" fisheye lens used in Nikon Coolpix8700. This comparison is given in Table 3 and the resulting graphics are shown in Figures 8 and 9.

Since A_3 distorsion parameter was a so small value that can be ignored, it was not analyzed and written in Table 3. Table 3 shows that the significance values of the iPhone are higher than that of Nikon because of smaller pixel (they are given in Table 1) structure of iPhone's camera.

When Figure 8 is examined, it is seen that distortion parameters of iPhone 4S camera and Olloclip 3 in one fisheye lens equipment are larger, although they have a larger focal length. It does not show a significant difference compared to Nikon Coolpix8700 camera and FC-09 fisheye lens equipment. (c_k: focal length after calibration process, x_0: image

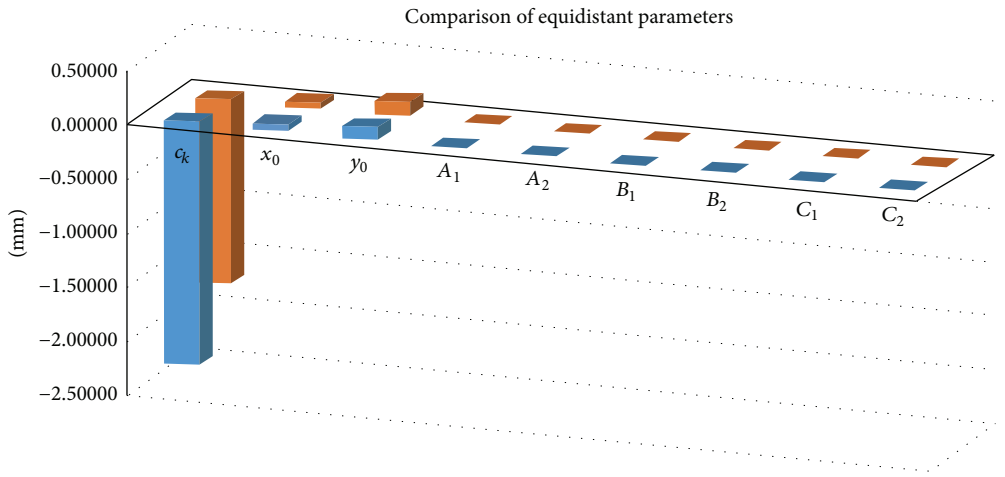

	c_k	x_0	y_0	A_1	A_2	B_1	B_2	C_1	C_2
Olloclip 3 in one	−2.23950	0.05886	0.10471	0.00080	−0.00386	−0.00105	−0.00137	0.00051	−0.00038
Nikon FC-E9	−1.69005	0.03987	0.11442	0.00119	−0.00068	−0.00026	0.00021	−0.00010	0.00032

Figure 8: Distortion parameters for two different camera fisheye lens combinations.

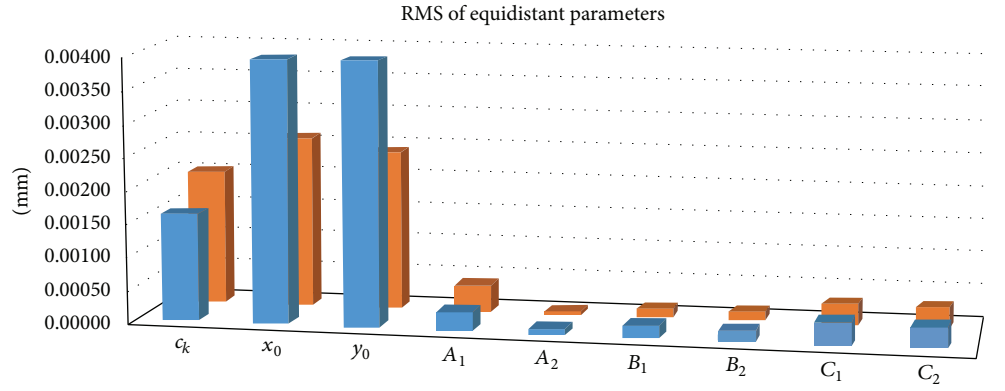

	c_k	x_0	y_0	A_1	A_2	B_1	B_2	C_1	C_2
Olloclip 3 in one	0.00161	0.00397	0.00399	0.00027	0.00007	0.00017	0.00015	0.00033	0.00031
Nikon FC-E9	0.00203	0.00259	0.00240	0.00039	0.00005	0.00013	0.00012	0.00029	0.00028

Figure 9: Root mean square values of distortion parameters for two different camera fisheye lens combinations.

coordinate of principle point in X direction, and y_0: image coordinate of principle point in Y direction).

Figures 8 and 9 illustrate that when x_0, y_0 principal image point coordinate values and focal lengths of two different fisheye lens are ignored for the cameras with the same resolution and the same pixel size, a meaningful approximation is obtained. In consideration of these results, current technology developed for Olloclip 3 in one lens that is improved for mobile phones is particularly great. Nikon FC-E9 mounted on bulky Nikon Coolpix8700 is difficult to use. Olloclip 3 in one lens mounted on iPhone 4S is considered to be used in studies done with photogrammetric fisheye lens instead of Nikon FC-E9. The conclusion part compares the advantages and disadvantages of two different fisheye images.

Nine of 112 control points are considered as passing points, while 103 of them are full control points. 103 point coordinates from testing area are considered errorless and used in bundle block adjustment. Three-dimensional position data derived from the bundle block adjustment are compared to the errorless points. Nikon Coolpix8700 camera and FC-09 fisheye lens combination gives accuracy on 85 points under the subpixel level. iPhone 4S camera and Olloclip 3 in one fisheye lens combination gives accuracy on 89 points under the subpixel level. This means that there is 82.52% accuracy for Nikon Coolpix8700 camera and FC-09 fisheye lens combination and 86.40% accuracy for iPhone 4S camera and Olloclip 3 in one fisheye lens combination.

The coordinates of three-dimensional object coordinates of 103 points are subtracted from the points which derived

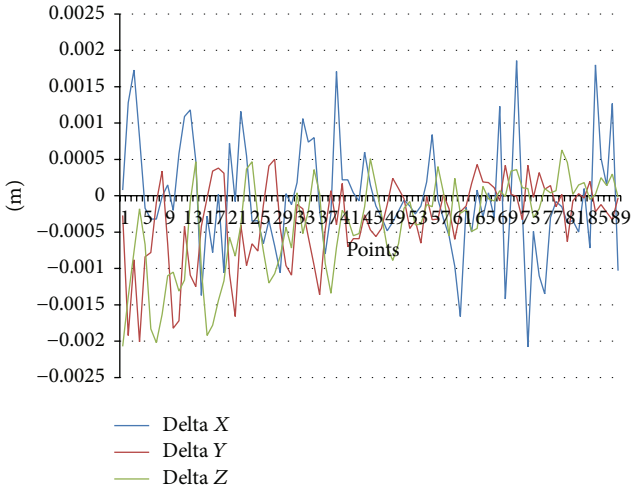

Figure 10: Subpixel graphic for the combination of iPhone 4S camera with Olloclip 3 in one fisheye lens.

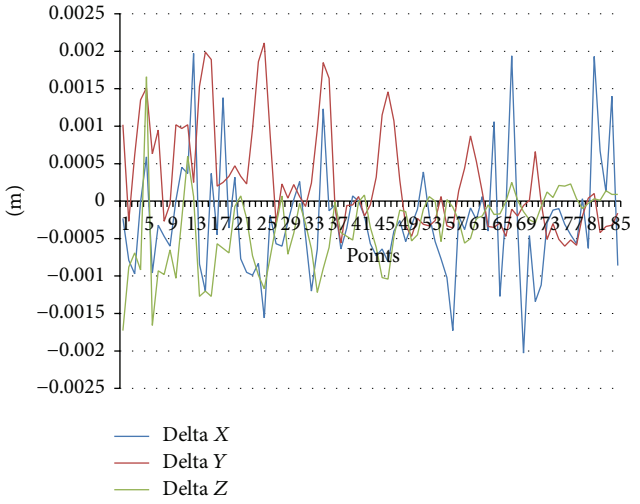

Figure 11: Subpixel graphic for the combination of Nikon Coolpix8700 camera with Nikon FC-E9 fisheye lens.

from bundle block adjustment process. If the difference values are greater than subpixel level in any axis then they are eliminated; consequently Figures 10 and 11 are depicted from the obtained differences, respectively, for iPhone 4S camera and Olloclip 3 in one fisheye lens combination and Nikon Coolpix8700 camera and FC-09 fisheye lens combination. Delta X is the difference between three-dimensional point coordinate which is measured before adjustment in X direction and three-dimensional point coordinate which is derived after adjustment in X direction. Delta Y and delta Z were calculated similarly.

The standard deviations of coordinate differences have been calculated for three different axes from the data contributing to depicting Figures 10 and 11. The standard deviation values on the X, Y, and Z axes are 0.763 mm, 0.558 mm, and 0.638 mm, respectively, for Olloclip 3 in one lens kit. By using similar derivation, the standard deviation values on the X, Y, and Z axes are 0.748 mm, 0.699 mm, and 0.517 mm, respectively, for Nikon FC-09 lens kit. As presented, the standard deviation values of identical axes are found approximately close to each other from the calculations. Moreover, when the distribution of the coordinate differences was evaluated for three identical axes (X, Y, Z) of these two kinds of lens kits, it was calculated that they have the same maximum difference value which is approximately 2 mm. From these graphics, root mean square error of point positions has been determined as 3.556 mm for Olloclip 3 in one and 3.401 mm for Nikon FC-09 lens kit. These values show that the internal reliability of these two kinds of fisheye lens kits are similar for three-dimensional point coordinate determination.

Advantages and disadvantages of using fisheye lenses for the abovementioned equipment can be listed as follows.

Advantages

(i) iPhone 4S camera and Olloclip 3 in one fisheye lens equipment is lightweight and is much more easy to use.

(ii) As given in Table 3, focal distance of iPhone 4S camera and Olloclip 3 in one fisheye lens equipment is larger than focal distance of Nikon Coolpix8700 camera and FC-09 fisheye lens equipment. Root mean square of the larger focal distance is smaller than the other one.

(iii) There is no significant difference between the image center point coordinates of iPhone 4S camera and Olloclip 3 in one fisheye lens equipment and Nikon Coolpix8700 camera and FC-09 fisheye lens.

Disadvantages

(i) Nikon Coolpix8700 camera and FC-09 fisheye lens equipment is heavier and much more difficult to use.

(ii) Since focal distance of iPhone 4S camera and Olloclip 3 in one fisheye equipment is larger than Nikon Coolpix8700 camera and FC-09 fisheye lens equipment, the resulting distortion parameters are expected to be smaller and when distortion parameters of both equipment are compared to each other, there happens to be a stable result that exceeds the expectations.

(iii) As given in Table 3, mean square error values for image central point of iPhone 4S camera and Olloclip 3 in one fisheye lens equipment are higher than mean square error values of Nikon Coolpix8700 camera and FC-09 fisheye lens equipment. Therefore, Nikon Coolpix8700 camera and FC-09 fisheye lens equipment can be considered more stable.

(iv) iPhone 4S camera and Olloclip 3 in one fisheye lens equipment should be tested in a photogrammetric study and the results should be interpreted in the light of these data.

5. Conclusion

The main purpose of this study is to test fisheye lens equipment used with mobile phones. In this study, the performance of Olloclip 3 in one fisheye lens used with iPhone 4S mobile phone and Nikon FC-E9 fisheye lens used with Nikon Coolpix8700 camera is analyzed comparing the calibration results based on an equidistant model. The calibration parameters were found to be approximate for these two kinds of hardware. The resolutions of the cameras are the same for these two kinds of hardware. The coordinates of image center point were found approximately close to each other from the calculations for these two kinds of hardware. It was seen that the calibration results of Olloclip 3 in one fisheye lens used with iPhone 4S mobile phone have not shown statistical significant difference results compared to Nikon FC-E9 fisheye lens used with Nikon Coolpix8700. Also it was seen from the results of this study that Olloclip 3 in one fisheye lens has larger focal length than the other.

In the near future, iPhone 4S camera and Olloclip 3 in one fisheye lens and Nikon Coolpix8700 equipment are going to be tested in a photogrammetric case study. In compliance with the results of this study, it is expected from the photogrammetric measurement results that Olloclip 3 in one fisheye lens used with iPhone 4S mobile phone will not show statistical significant difference results compared to Nikon FC-E9 fisheye lens used with Nikon Coolpix8700 which will be used for photogrammetric measurement assessments; besides having larger focal length it is expected to give better results than Nikon FC-E9 fisheye lens used with Nikon Coolpix8700. This experimental study shows that Olloclip 3 in one fisheye lens developed for mobile phones has at least similar characteristics with classic fisheye lenses.

Competing Interests

The author declares that there are no competing interests.

Acknowledgments

In this publication, bundle block adjustment software developed by Dr. Danilo Schneider in Germany Dresden Technical University has been used. The author hereby is thankful to Dr. Ing. Danilo Schneider for the permission of software which was developed by him.

References

[1] iPhone Lens Kits Reviews, 2015, http://iphone-lens-kits-review.toptenreviews.com/.

[2] "olloclip," 2015, https://www.olloclip.com/.

[3] A. Gruen and D. Akca, "Calibration and accuracy testing of mobile phone cameras," in *Proceeding of the 28th Asian Conference on Remote Sensing (ACRS '07)*, pp. 1171–1177, Kuala Lumpur, Malaysia, November 2007.

[4] U. Aydar, *Comparison of photogrammetric and visualizations methods in obtaining façade plan [M.S. thesis]*, Istanbul Technical University Graduate School of Science Engineering and Technology, Istanbul, Turkey, 2007.

[5] D. Yamamoto, S. Ozeki, and N. Takahashi, "Wired fisheye lens: a motion-based improved fisheye interface for mobile web map services," in *Web and Wireless Geographical Information Systems: 9th International Symposium, W2GIS 2009, Maynooth, Ireland, December 7–8, 2009. Proceedings*, vol. 5886 of *Lecture Notes in Computer Science*, pp. 153–170, Springer, Berlin, Germany, 2009.

[6] S. Abraham and W. Förstner, "Fish-eye-stereo calibration and epipolar rectification," *ISPRS Journal of Photogrammetry and Remote Sensing*, vol. 59, no. 5, pp. 278–288, 2005.

[7] D. Gledhill, G. Y. Tian, D. Taylor, and D. Clarke, "Panoramic imaging—a review," *Computers & Graphics*, vol. 27, no. 3, pp. 435–445, 2003.

[8] E. Schwalbe, "Geometric modelling and calibration of fisheye lens camera systems," in *Proceedings of the 2nd Panoramic Photogrammetry Workshop, International Archives of Photogrammetry, Remote*, pp. 5–8, Berlin, Germany, February 2005.

[9] J. Kumler and M. Bauer, "Fisheye lens designs and their relative performance," in *Proceedings of the Current Developments in Lens Design and Optical Systems Engineering (SPIE '00)*, vol. 4093, pp. 360–369, San Diego, Calif, USA, October 2000.

[10] P. Dhane, K. Kutty, and S. Bangadkar, "A generic non-linear method for fisheye correction," *International Journal of Computer Applications*, vol. 51, no. 10, pp. 58–65, 2012.

[11] M. Yamashita, M. Yoshimura, and T. Nakashizuka, "Cloud cover estimation using multitemporal hemisphere imageries," in *Proceedings of the Photogrammetry and Remote Sensing, 20th ISPRS Congress, Commission VII, WG VII/6 (ISPRS '04)*, pp. 826–829, Istanbul, Turkey, 2004.

[12] L. Wang, F. Duan, and K. Lv, "Fisheye-lens-based visual sun compass for perception of spatial orientation," *Mathematical Problems in Engineering*, vol. 2012, Article ID 460430, 15 pages, 2012.

[13] J. K. W. Oh and J. S. Haberl, "New educational software for teaching the sunpath diagram and shading mask protractor," in *Proceedings of the 5th International IBPSA Conference: Building Simulation (ESL-PA-97/09-01)*, vol. 3–9, 7 pages, Prague, Czech Republic, September 1997.

[14] G. Krishnan and S. K. Nayar, "Cata-fisheye camera for panoramic imaging," in *Proceedings of the IEEE Workshop on Applications of Computer Vision (WACV '08)*, pp. 1–8, Copper Mountain, Colo, USA, January 2008.

[15] B. Streckel, J. F. Evers-Senne, and R. Koch, "Lens model selection for a markerless AR tracking system," in *Proceedings of the 4th IEEE and ACM International Symposium on Mixed and Augmented Reality*, pp. 130–133, Vienna, Austria, October 2005.

[16] X. Brun, J. E. Deschaud, and F. Goulette, "On-the-way city mobile mapping using laser range scanner and fisheye camera," in *Proceedings of the 5th International Symposium on Mobile Mapping Technology (MMT '07)*, vol. 8, 8 pages, Padua, Italy, May 2007.

[17] A. Ahmad and P. Lima, "Multi-robot cooperative spherical-object tracking in 3D space based on particle filters," *Robotics and Autonomous Systems*, vol. 61, no. 10, pp. 1084–1093, 2013.

[18] J. Y. Zheng and S. Li, "Employing a fish-eye for scene tunnel scanning," in *Proceedings of the 7th Asian Conference on Computer Vision (ACCV '06)*, P. J. Narayanan, S. K. Nayar, and H.-Y. Shum, Eds., vol. 3851 of *Lecture Notes in Computer Science*, pp. 509–518, Hyderabad, India, January 2006.

[19] E. Martinez and A. P. Del Pobil, "A dioptric stereo system for robust real-time people tracking," in *Proceeding of the Workshop*

on People Detection and Tracking in IEEE International Conferance on Robotics and Automation (ICRA '09), Kobe, Japan, May 2009.

[20] A. Gurtner, *Investigsation of fisheye lenses for small UAV aerial photography [M.S. thesis]*, Queensland University of Technology, Brisbane, Australia, 2008.

[21] B. Grelsson, *Global pose estimation from aerial images registration with elevation models [Ph.D. thesis]*, Linköping University Electronic Press, Linköpings Universitet, Linköping, Swedish, 2014.

[22] T. Naruse, T. Kaneko, A. Yamashita, and H. Asama, "3-D measurement of objects in water using fish-eye stereo camera," in *Proceeding of the 19th IEEE International Conference on Image Processing (ICIP '12)*, pp. 2773–2776, Orlando, Fla, USA, October 2012.

[23] S. Bouaziz, *Geolocalization using skylines from omni-images [M.S. thesis]*, Virtual Reality Laboratory, École Polytechnique Fédérale de Lausanne, Lausanne, Switzerland, 2009.

[24] A. Georgantas, M. Brédif, and M. P. Desseilligny, "An accuracy assessment of automated photogrammetric techniques for 3D modelling of complex interiors," in *Proceeding of 22th The International Archives of the Photogrammetry, Remote Sensing and Spatial Information Sciences (ISPRS '12)*, vol. 39-B3, pp. 23–28, Melbourne, Australia, September 2012.

[25] D. Schneider and E. Schwalbe, "Integrated processing of terrestrial laser scanner data and fisheye-camera image data," in *Proceedings of the 21st ISPRS Congres*, pp. 1037–1044, Beijing, China, July 2008.

[26] C. Hughes, P. Denny, E. Jones, and M. Glavin, "Accuracy of fish-eye lens models," *Applied Optics*, vol. 49, no. 17, pp. 3338–3347, 2010.

[27] J. M. Junior, M. V. A. Moraes, and A. M. G. Tommaselli, "Experimental assessment of techniques for fisheye camera calibration," *Boletim de Ciências Geodésicas*, vol. 21, no. 3, pp. 637–651, 2015.

[28] D. Schneider, E. Schwalbe, and H.-G. Maas, "Validation of geometric models for fisheye lenses," *ISPRS Journal of Photogrammetry and Remote Sensing*, vol. 64, no. 3, pp. 259–266, 2009.

[29] J. Kannala and S. S. Brandt, "A generic camera model and calibration method for conventional, wide-angle, and fish-eye lenses," *IEEE Transactions on Pattern Analysis and Machine Intelligence*, vol. 28, no. 8, pp. 1335–1340, 2006.

[30] J. A. Parian, "Panoramic imaging: techniques, sensor modeling and applications," in *Proceedings of the International Summer School on "Digital Recording and 3D Modelling"*, Crete, Greece, April 2006.

[31] S. Thirthala and M. Pollefeys, "The radial trifocal tensor: a tool for calibrating the radial distortion of wide-angle cameras," in *Proceedings of the IEEE Computer Society Conference on Computer Vision and Pattern Recognition (CVPR '05)*, vol. 1, pp. 321–328, San Diego, Calif, USA, June 2005.

[32] C. Hughes, M. Glavin, and E. Jones, "Simple fish-eye calibration method with accuracy evaluation," *Electronic Letters on Computer Vision and Image Analysis*, vol. 10, no. 1, pp. 54–62, 2011.

[33] K. B. Johnson, *Development of a versatile wide-angle lens characterization strategy for use in the OMNIster stereo vision system [M.S. thesis]*, University of Tennessee, Knoxville, Tenn, USA, 1997.

[34] K. Miyamoto, "Fish eye lens," *Journal of the Optical Society of America*, vol. 54, no. 8, pp. 1060–1061, 1964.

[35] M. Yamashita, M. Yoshimura, and T. Nakashizuka, "Cloud cover estimation using multitemporal hemisphere imageries," in *Proceedings of the International Society for Photogrammetry and Remote Sensing*, vol. 35, pp. 826–829, Istanbul, Turkey, 2004.

[36] C. Hughes, P. Denny, M. Glavin, and E. Jones, "Equidistant fish-eye calibration and rectification by vanishing point extraction," *IEEE Transactions on Pattern Analysis and Machine Intelligence*, vol. 32, no. 12, pp. 2289–2296, 2010.

[37] C. Hughes, R. McFeely, P. Denny, M. Glavin, and E. Jones, "Equidistant ($f\theta$) fish-eye perspective with application in distortion centre estimation," *Image and Vision Computing*, vol. 28, no. 3, pp. 538–551, 2010.

[38] S. Parhizgar, *An evaluation of an omni-directional (fisheye) vision sensor for estimating the pose of an object [M.S. thesis]*, University of Regina, Master of Applied Science in Software Systems Engineering University of Regina, Saskatchewan, Canada, 2014.

[39] Nikon, 2015, http://imaging.nikon.com/.

[40] Image Resource, 2015, http://www.imaging-resource.com/.

[41] "photo.net," 2015, http://photo.net/.

[42] C. Sahin, *A construction of camera calibration field for close range photogrammetric camera calibration [M.S. thesis]*, Gebze Institute of Technology, Graduate School of Science Engineering and Sciences, Kocaeli, Turkey, 2004.

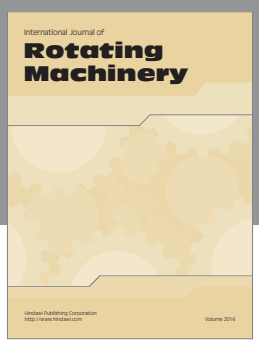

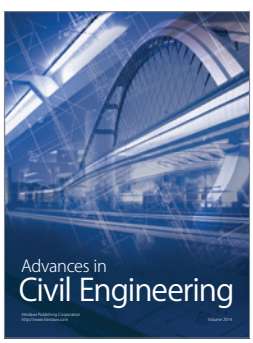

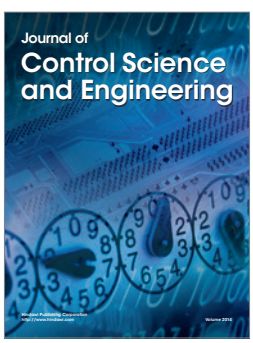

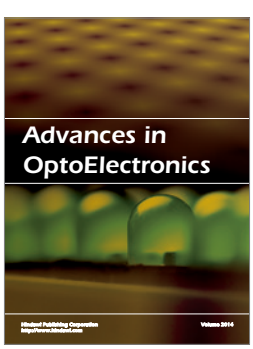

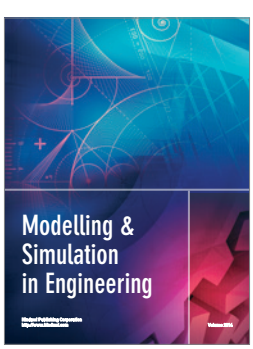

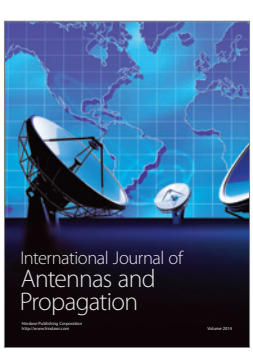

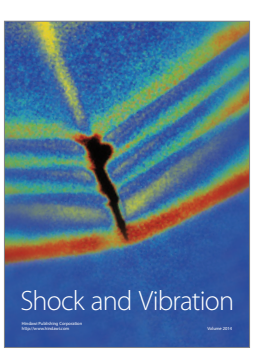

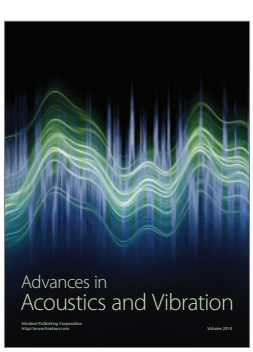

Hindawi

Submit your manuscripts at
http://www.hindawi.com